Available online at www.sciencedirect.com
SCIENCE DIRECT®
ELSEVIER
International Journal of Heat and Mass Transfer 48 (2005) 2625–2634
International Journal of HEAT and MASS TRANSFER
www.elsevier.com/locate/ijhmt

Analysis of surface roughness effects on heat transfer in micro-conduits

J. Koo, C. Kleinstreuer *

North Carolina State University, Department of Mechanical and Aerospace Engineering, Campus Box 7910 Raleigh, NC 27695-7910, USA

Received 25 December 2004; received in revised form 31 January 2005
Available online 1 April 2005

Abstract

Modern heat rejection systems, such as micro-heat sinks, are attractive because of their potential for high performance at small size and low weight. However, the impact of microscale effects on heat transfer have to be considered and quantitatively analyzed in order to gain physical insight and accurate Nusselt number data. The relative surface roughness (SR) was selected as a key microscale parameter, represented by a porous medium layer (PML) model. Assuming steady laminar fully developed liquid flow in microchannels and microtubes, the SR effects in terms of PML thermal conductivity ratio and Darcy number on the dimemsionless temperature profile and Nusselt number were analyzed. In summary, the PML characteristics, especially the SR-number and conductivity ratio k_m/k_f, greatly affect the heat transfer performance where the Nusselt number can be either higher or lower than the conventional value. The PML influence is less pronounced in microtubes than in parallel-plate microchannels.

Keywords: Thermal flow; Microchannels; Microtubes; Computational analyses; Microscale parameters; Dimensionless temperature profiles; Nusselt numbers

1. Introduction

The compactness and high surface-to-volume ratio of microscale fluid flow devices, such as micro-heat-sinks, make them attractive alternatives to conventional systems. However, recent reviews of experimental and computational studies of liquid flow in microchannels pointed out that microscale effects, such as surface roughness, are the cause for discrepancies between observed and actual values of, say, the friction factor and convection heat transfer coefficient. For example, Koo and Kleinstreuer [1] analyzed and classified experimental observations of friction factors into three groups. They suggested possible causes resulting in deviation from the conventional, i.e., macroscale, observations, including entrance effects, wall slip effects, surface roughness, and viscous dissipation. The surface roughness (SR) effect, i.e., $1 \leqslant \text{SR} \leqslant 4\%$ (see Table 1), appears to be dominant, where the friction factor could either increase or decrease depending on the SR characteristics [2]. Specifically, Kleinstreuer and Koo [2] introduced a porous medium layer (PML) model to investigate numerically the effects of surface roughness on the friction factor in microchannels. In more detail, Croce and D'Agaro

* Corresponding author. Tel.: +1 919 5155261; fax: +1 919 5157968.
E-mail address: ck@eos.ncsu.edu (C. Kleinstreuer).

0017-9310/$ - see front matter
doi:10.1016/j.ijheatmasstransfer.2005.01.024

Nomenclature

c	specific heat [J/kg K]
c	drag coefficient [–]
C	constant [–]
d	diameter [m]
D	channel diameter [m]
Da	Darcy number [–]
h	heat transfer coefficient [W/m^{2}K]
H	channel height [m]
k	thermal conductivity [W/m K]
Nu	Nusselt number [–]
p	pressure [N/m^2]
PML	Porous Medium Layer
Pr	Prandtl number [–]
q	heat flux [W/m^2]
Re	Reynolds number [–]
SR	(relative) surface roughness [–]
T	temperature [K]
U_0	inlet velocity [m/s]
w	interparticle potential [J]
x	axial coordinate [m]
y	transversal or radial coordinate [m]

Greek symbols

β	slip coefficient [–]
κ	permeability [m^2]
μ	dynamic viscosity [N s/m^2]
ρ	density [kg/m^3]
ϕ	volume fraction [–]
θ	dimensionless temperature [–]

Superscript

*	dimensionless quantities

Subscripts

0	mean inlet value
c	continuous phase
d	discrete phase
f	fluid
h	hydraulic
int	at interface
l	liquid phase
m	mass flux mean value for liquid phase
m	mean value in PML
n	normal component
s	solid (wall) phase
s	PML thickness
w	wall ($y = 0$)
ξ	y-coordinate of the interface between porous medium layer and clear region

Table 1
Typical values of relative surface roughness ($h/D_h \times 100$[%])

Author	Relative surface roughness [%]	Material
Pfhaler et al. [12]	~1	Silicon
Peng et al. [13]	~0.6–1	Silicon
Mala and Li [14]	~3.5	Stainless steel/fused silica
Papautsky et al. [15]	~2	Silicon
Xu et al. [16,17]	~1–1.7	Aluminum, silicon

[3] analyzed SR-effects on the friction factor and Nusselt number for parallel plate channels and tubes with triangular and rectangular surface roughness elements. They observed vortex structures behind the roughness elements resulting in a friction factor increase for both conduits. However, while the Nusselt number increased for parallel plates it decreased for thermal flow in tubes. Overall, they observed that the Nusselt number is less sensitive to surface roughness effects than the friction factor is. Unfortunately, they did not include the effect of thermal conductivity ratio between the roughness elements and bulk fluid, subject to only the constant wall temperature condition. Furthermore, their roughness elements were two dimensional (axi-symmetric), which deviates from actual cases.

Sobhan and Garimella [4] reviewed published experimental data on fluid flow and heat transfer in microchannels, and summarized that the possible causes of the discrepancies in prediction could be entrance and exit effects, differences in surface roughness in the different microchannels investigated, non-uniformities in channel dimensions, nature of the thermal and flow boundary conditions, as well as uncertainties and errors in instrumentation, measurement, and measurement location. Morini [5] added electro-osmotic effects (EDL) to the list of possible causes.

Kuznetsov and Xiong [6] stated that the Nusselt number was a function of Darcy number, Forchheimer number, Reynolds number, and interface position. Subsequently, Kuznetsov [7] reported that during convection in a porous medium, there may be significant heat transfer due to mixing of the interstitial fluid at the pore scale in addition to the molecular diffusion of heat, an effect called thermal dispersion.

In addition to surface roughness, wall-slip and possible two-phase effects in microchannels were discussed by several researchers. For example, Tretheway and Meinhart [8] observed a wall-slip velocity for water flow on hydrophobic walls, while Wu and Cheng [9] measured a decrease of Nusselt number for flows in hydrophobic channels and an increase in channels of high relative surface roughness. Tyrrell and Attart [10] reported the existence of 20–30 (nm) thick air bubble gaps between wall and bulk water using atomic force microscopy, and Tretheway and Mainhart [11] calculated the necessary air gap thickness to yield the velocity slip they observed. As expected, the existence of an air gap will decrease the heat transfer performance in channels.

Clearly, momentum and heat transfer in microchannels are results of complex physical phenomena. In the current study, the PML model employed by Kleinstreuer and Koo [2] is expanded to investigate the surface roughness effects on heat transfer phenomena for liquid flow in hydrophilic conduits, i.e., microchannels and microtubes.

2. Theory

The general governing equations for momentum and energy transfer in conduits with PMLs read

$$\rho \frac{D\vec{u}}{Dt} = -\nabla p + \nabla \cdot \tau_{ij} - \{(R_C + R_F|\vec{u}|)\vec{u}\}_{\mathrm{PML}} \tag{1}$$

$$\rho c_p \frac{DT}{Dt} = \{\nabla \cdot (k_f \nabla T)\}_{\mathrm{clear}} + \left\{\nabla \cdot \left(\left(k_m + Ck_f Pr \frac{\rho_f u_f d_p}{\mu_f}\right)\nabla T\right)\right\}_{\mathrm{PML}} \tag{2}$$

Assuming steady laminar fully developed viscous flow in a parallel-plate microchannel with porous medium layer (see Fig. 1), the governing equations can be presented as

$$-\frac{dp}{dx} + \mu_f \frac{d^2 u_f}{dy^2} = 0, \quad 0 \leqslant y \leqslant \xi \tag{3}$$

$$-\frac{dp}{dx} + \mu_{\mathrm{eff}} \frac{d^2 u_f}{dy^2} - \frac{\mu_f}{\kappa} u_f - \frac{\rho_f c_F}{\kappa^{1/2}} u_f^2 = 0 \quad \xi \leqslant y \leqslant \xi + s \tag{4}$$

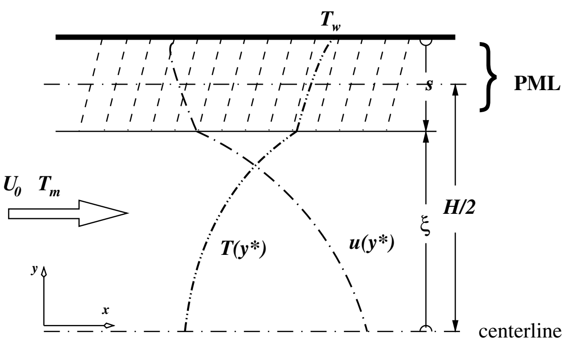

Fig. 1. Schematics of the problem.

$$\rho_f c_f u_f \frac{\partial T}{\partial x} = k_f \frac{\partial^2 T}{\partial y^2}, \quad 0 \leqslant y \leqslant \xi \tag{5}$$

$$\rho_f c_f u_f \frac{\partial T}{\partial x} = \frac{\partial}{\partial y}\left[\left(k_m + Ck_f Pr \frac{\rho_f u_f d_p}{\mu_f}\right)\frac{\partial T}{\partial y}\right] \xi \leqslant y \leqslant \xi + s \tag{6}$$

Eq. (3) is the momentum equation for the clear fluid region while Eq. (4) holds for the porous region (i.e., the Brinkman–Forchheimer-extended Darcy equation). Eqs. (5) and (6) are the energy equations for the clear fluid and porous region, respectively. The energy equation for the porous region accounts for transverse thermal dispersion, while longitudinal thermal dispersion is neglected. This is consistent with the assumption of longitudinal conduction, $k_x \partial^2 T/\partial x^2$ being negligible in comparison with $k_y \partial^2 T/\partial y^2$.

The thermal dispersion term $Ck_f Pr \frac{\rho_f u_f d_p}{\mu_f}$ can be rewritten as

$$Ck_f Pr \frac{\rho_f u_f d_p}{\mu_f} = Ck_f Pr Re_p = Ck_f Pr Re_{D_h} \frac{u_f}{U_0} \frac{d_p}{D_h} \tag{7}$$

Eqs. (3)–(6) are subject to the following boundary conditions:

$$\frac{\partial u_f}{\partial y} = 0 \quad \text{at } y = 0 \tag{8}$$

$$\frac{\partial T}{\partial y} = 0 \quad \text{at } y = 0 \tag{9}$$

$$u|_{y=\xi-0} = u|_{y=\xi+0} \quad \text{at } y = \xi \tag{10}$$

$$\mu_{\mathrm{eff}} \left.\frac{\partial u_f}{\partial y}\right|_{y=\xi+0} - \mu_f \left.\frac{\partial u_f}{\partial y}\right|_{y=\xi-0} = \beta \frac{\mu_f}{\kappa^{1/2}} u_f\Big|_{y=\xi} \quad \text{at } y = \xi \tag{11}$$

$$T|_{y=\xi+0} = T|_{y=\xi-0} \quad \text{at } y = \xi \tag{12}$$

$$\left(k_m + Ck_f Pr \frac{\rho_f u_f d_p}{\mu_f}\right) \left.\frac{\partial T}{\partial y}\right|_{y=\xi+0} = k_f \left.\frac{\partial T}{\partial y}\right|_{y=\xi-0} \quad \text{at } y = \xi \tag{13}$$

$$u_f = 0 \quad \text{at } y = \xi + s \tag{14}$$

$$\left(k_m + Ck_f Pr \frac{\rho_f u_f d_p}{\mu_f}\right) \frac{\partial T}{\partial y} = q'' \quad \text{at } y = \xi + s \tag{15}$$

For the mean (or effective) PML conductivity, Kuznetsov and Xiong [6] used the relation

$$k_m = \phi k_f + (1 - \phi) k_s \tag{16}$$

In the current study, β the slip coefficient was assumed to be zero.

After non-dimensionalization, the governing equations read

$$u^* Nu = -4 \frac{d^2\theta}{dy^{*2}} \tag{17}$$

$$u^{*}Nu = -4\left[\left(\frac{k_{\mathrm{m}}}{k_{\mathrm{f}}}\right) + CPrRe_{\mathrm{p}}\right]\frac{\mathrm{d}^{2}\theta}{\mathrm{d}y^{*2}} \tag{18}$$

where $u^{*} = u_{\mathrm{f}}/U_{0}$, $Nu = h \cdot 2H/k_{\mathrm{f}}$, $\theta = (T_{\mathrm{m}} - T)/(T_{\mathrm{m}} - T_{w})$, $Pr = \mu/\rho\alpha$, and $Re_{\mathrm{p}} = \rho_{\mathrm{f}}u_{\mathrm{f}}d_{\mathrm{p}}/\mu$. Here, U_{0} is the mean velocity, h is the heat transfer coefficient, and d_{p} represents the equivalent hydraulic diameter of the surface roughness elements. For a porous-medium free, i.e., clear part of the microchannel

$$u^{*}(y^{*}) = \frac{Re_{D_{\mathrm{h}}}}{4}\frac{\mathrm{d}p^{*}}{\mathrm{d}x^{*}}(y^{*} - \xi^{*2}) + u^{*}_{\mathrm{int}} \tag{19}$$

where ξ^{*} is the non-dimensionalized coordinate for the open channel-porous medium layer interface, and u^{*}_{int} is the flow velocity at the interface, which depends on the iterative solution to the PML-flow problem.

The dispersion term was found to be negligible because the velocity in the surface roughness region is very small, implying very low particle Reynolds numbers. Referring to Kleinstreuer and Koo [2], typical values of $\frac{u_{\mathrm{f}}}{U_{0}}$ and $\frac{d_{\mathrm{p}}}{D_{\mathrm{h}}}$ are in the order of $\mathcal{O}(10^{-1})$ and $\mathcal{O}(10^{-2})$, respectively. Considering typical values of C, Pr and $Re_{D_{\mathrm{h}}}$ to be 0.1, 5 and 2000, respectively, the order of magnitude of the thermal dispersion term is in the order of k_{f}, which can be usually neglected due to high $k_{\mathrm{s}}/k_{\mathrm{f}}$ ratios and hence high $k_{\mathrm{m}}/k_{\mathrm{f}}$ values. According to Kuznetsov [7], the thermal dispersion effect is negligible for $Re_{\mathrm{p}} < 100$. For the present case, $Re_{\mathrm{p \cdot max}} = 1$ and hence the thermal dispersion effect will be neglected. However, it becomes important for fluid flows of high Prandtl numbers, such as oils ($Pr \sim 1000$).

For the clear region, Eq. (17) can be integrated with the given parabolic velocity profile to:

$$\theta = \left\{\frac{Re_{D_{\mathrm{h}}}}{4}\frac{\mathrm{d}p^{*}}{\mathrm{d}x^{*}}\left(\frac{1}{12}y^{*4} - \frac{1}{2}y^{*2}\xi^{*2} + \frac{5}{12}\xi^{*4}\right) + \frac{1}{2}u^{*}_{\mathrm{int}}\left(y^{*2} - \xi^{*2}\right)\right\}Nu + \theta_{\mathrm{int}} \tag{20}$$

The velocity profiles were obtained in the same way as introduced in Kleinstreuer and Koo [2], and the Nusselt numbers were iteratively obtained to meet the energy balance at the interface. 300 elements were evenly distributed in the porous medium layer and 2000 elements in the open region. The equations were solved using a boundary-value-problem ordinary differential equation solver routine that is provided in MATLAB 7.0.

3. Results and discussion

In order to gain a better understanding of convective heat transfer in microchannels with measurable surface roughness, $\mathrm{SR} \equiv s/D_{\mathrm{h}}$, the dependence of the Nusselt number on SR is established. By definition,

$$Nu = \frac{hD_{\mathrm{h}}}{k_{\mathrm{f}}} \tag{21a}$$

where

$$h = \frac{q''}{T_{\mathrm{w}} - T_{\mathrm{m}}} = \frac{k_{\mathrm{m}}(\mathrm{d}T/\mathrm{d}y)|_{\mathrm{wall}}}{T_{\mathrm{w}} - T_{\mathrm{m}}} \tag{21b}$$

For a given relative surface roughness, Eq. (21a) and (21b) are combined into

$$Nu \sim \frac{k_{\mathrm{m}}}{k_{\mathrm{f}}}\left.\frac{\mathrm{d}\theta}{\mathrm{d}y^{*}}\right|_{\mathrm{wall}} \tag{21c}$$

which can be rewritten for a given thermal conductivity ratio in the form:

$$Nu \sim \frac{k_{\mathrm{m}}}{k_{\mathrm{f}}}\left.\frac{\mathrm{d}\theta}{\mathrm{d}y^{*}}\right|_{\xi^{*}+0}\frac{1}{Re_{D_{\mathrm{h}}}f/6(1-\mathrm{SR}/2)^{3}} \tag{21d}$$

Of interest are the effects of SR characteristics in terms of the Darcy number, $Da = \frac{\kappa}{(H/2)^{2}}$ (or, $Da = \frac{\kappa}{R^{2}}$ for tubes), thermal conductivity ratio and Reynolds number on the Nusselt number, considering first parallel plates (Section 3.1) and then tubes (Section 3.2).

3.1. Parallel plates

3.1.1. Effects of Darcy number and PML thermal conductivity

The effect of PML thermal conductivity on the temperature profile in a channel is shown in Fig. 2, where $\theta \equiv \frac{T_{\mathrm{m}}-T}{T_{\mathrm{m}}-T_{\mathrm{w}}}$. The higher the PML thermal conductivity is, the lower is the centerline temperature to yield higher Nusselt numbers. The temperature profiles in the PML are affected by the thermal conductivity ratio more significantly at relatively low values compared to those at high ones. Fig. 3 illustrates the Darcy number effect on the temperature profiles, which turned out to be minimal. Clearly, the PML thermal conductivity affects temperature profiles more strongly than the Darcy number.

Fig. 4 shows the effects of PML Darcy number and thermal conductivity on the Nusselt number for the case of SR = 2% and $Re_{D_{\mathrm{h}}} = 1000$. As expected, the Nusselt number increased with an increase in PML conductivity. The Nusselt number showed deviations from the conventional laminar flow result ($Nu = 8.235$) between −4% and 9% depending on the PML characteristics. Specifically, the Nusselt number is lower than the conventional result, for low Darcy number and low thermal conductivity conditions, and it increases with elevated PML Darcy number and thermal conductivity values. The Nusselt number change is observed to be sensitive in the mid-range regime, i.e., $Da = 10^{-3}$ to 10^{-4}. Indeed, there is a relationship between the Darcy number and thermal conductivity, since the PML thermal conductivity depends on the void fraction which is directly related to the Darcy number. For certain types of porous media, the *Kozeny–Carman* equation could be used as the relation with void fraction, ϕ, i.e., $\kappa = \frac{\mathrm{d}^{2}\phi^{3}}{180(1-\phi)^{2}}$, although the

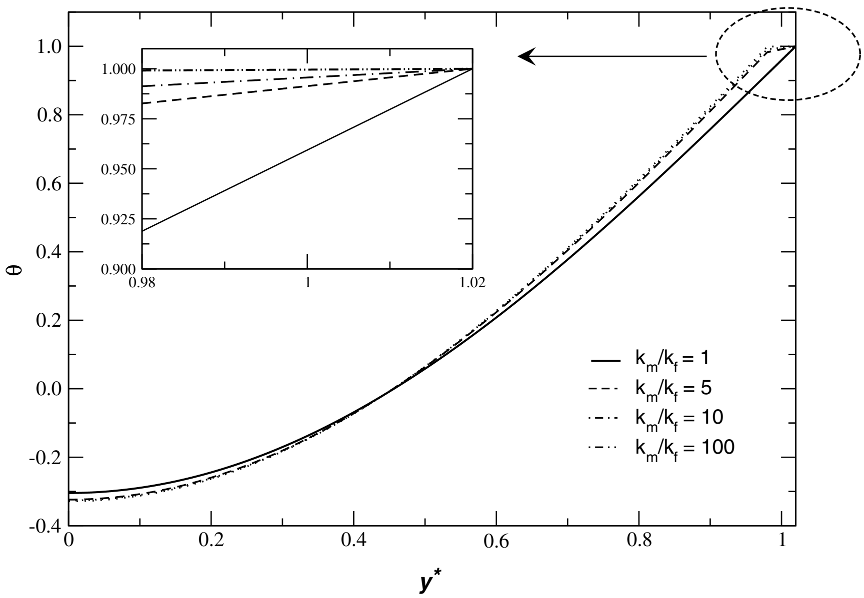

Fig. 2. PML thermal conductivity effect on the temperature profiles between parallel plates ($Da = 10^{-3}$, SR = 2%).

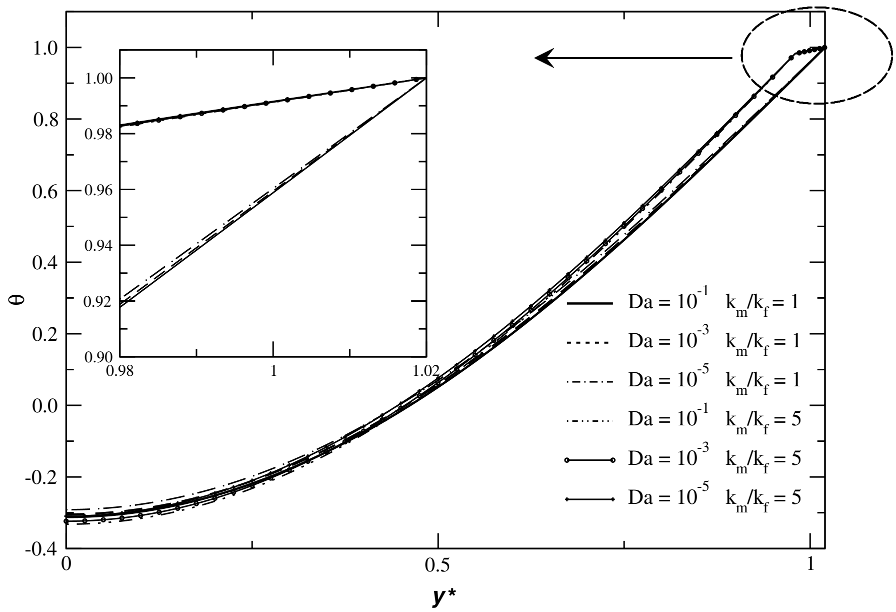

Fig. 3. Darcy number effect on the temperature profiles between parallel plates (SR = 2%).

surface roughness elements forming the PML are not exactly homogeneous and isotropic. The Reynolds number dependence is stronger in the mid-Darcy number range compared to that in low- and high-Darcy number ranges. The Nusselt number increases rapidly for low PML thermal conductivities, and it increases slowly under high thermal conductivity conditions. This indicates that there exists a limiting Nusselt number when increasing the PML thermal conductivity.

Judging from Figs. 3 and 4, the Darcy number influences convection more in the clear region than conduction in the surface roughness region for a given

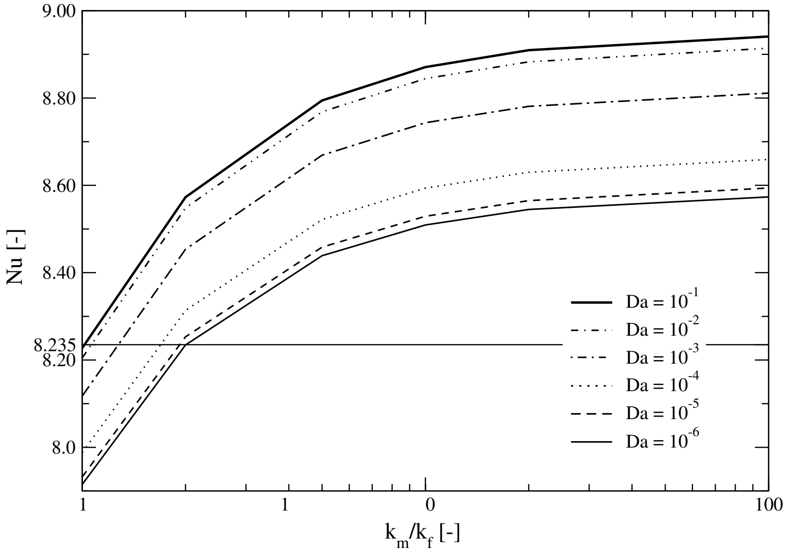

Fig. 4. Effects of PML Darcy number and thermal conductivity on the Nusselt number for parallel plates (Re = 1000, SR = 2%).

k_m/k_f-ratio. Specifically, the temperature profiles in Fig. 3 do not change much with the Darcy number in contrast to the Nusselt number (see Fig. 4).

As indicated in Eq. (21c), the Nusselt number is a function of the conductivity ratio and the temperature gradient at the wall. In Fig. 2, it was shown that the temperature gradient is greater for the lower conductivity cases, and it decreases fast with the thermal conductivity ratio; that explains the high rate of the Nusselt number increase at low thermal conductivity ratios. The temperature gradient at the wall increases with the Darcy number; thus, the Nusselt number increases with the Darcy number as shown in Fig. 4.

3.1.2. Reynolds number effect

Conventionally, the Nusselt number for laminar flow is independent of the Reynolds number. However, a weak Reynolds number dependence is observed for microchannels with PMLs, as shown in Fig. 5. Although the Reynolds number dependence is stronger in the Darcy number mid-range, overall its influence is usually negligible for $1 \leqslant \text{SR} \leqslant 4\%$.

3.1.3. Effect of relative surface roughness

Fig. 6 shows the SR effect, i.e., thickness of the PML, on the Nusselt number, where the Reynolds number is 1000 for all cases. The Nusselt number as a function of k_m/k_f varies only from 8.0927 to 8.5822 for SR = 1%, while it changes from 7.6378 to 9.6486 for SR = 4%. As the PML-thermal conductivity and surface roughness increase, the Nusselt number quickly exceeds the conventional value of 8.235. In more detail, for any given SR value, the thermal conductivity ratio decreases with the Darcy number for the cross-over point when $Nu \geqslant 8.235$.

When inspecting Eq. (21d), it is evident that the conductivity ratio and the temperature gradient have opposite impacts, assuming a constant relative surface roughness. In summary, the Nusselt number increases with relative surface roughness and decreases with the product of Reynolds number and friction factor.

3.2. Tubular flow

3.2.1. Effects of Darcy number and PML thermal conductivity

Compared to the parallel plate cases, the Nusselt number for tubes exceeds the conventional value of 4.365 at higher thermal conductivity ratios, as shown in Fig. 7. Specifically, the thermal conductivity ratio has to be increased by a factor of 10 to achieve the same Nusselt number improvement at low Darcy numbers. This could explain why most experimental Nusselt number data fall below the conventional value. For example, Croce and D'Agaro [3] reported that that Nusselt number is less sensitive to the roughness height with respect to the friction factor. Considering the friction factor changes with surface roughness as reported by Koo and Kleinstreuer [1] and the Nusselt number changes now given in Fig. 7, the observation of Croce and D'Agaro [3] can be confirmed. Furthermore, Croce and D'Agaro [3] reported an increase in Nusselt number for parallel plate flow and a decrease for tubular flow, which is evident when comparing Figs. 4 and 7.

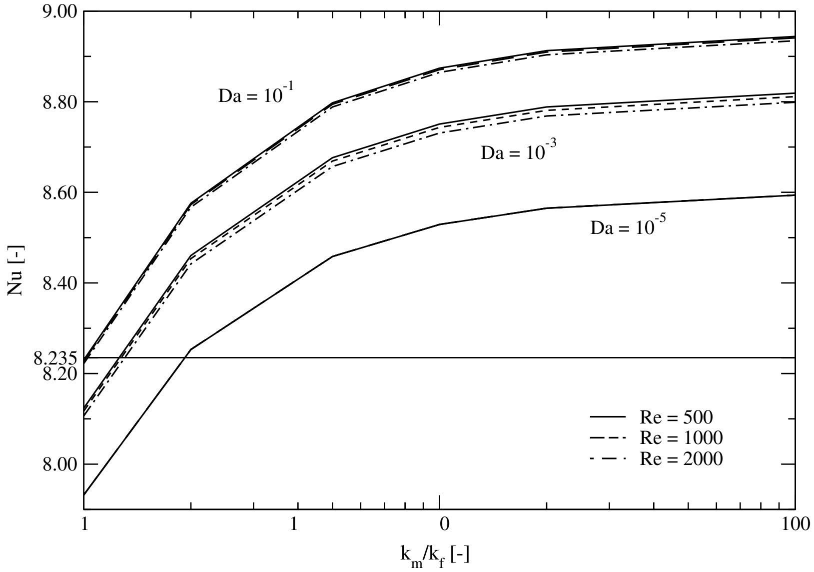

Fig. 5. Effect of the Reynolds number on the Nusselt number for different Darcy numbers and the conductivity ratios (SR = 2%).

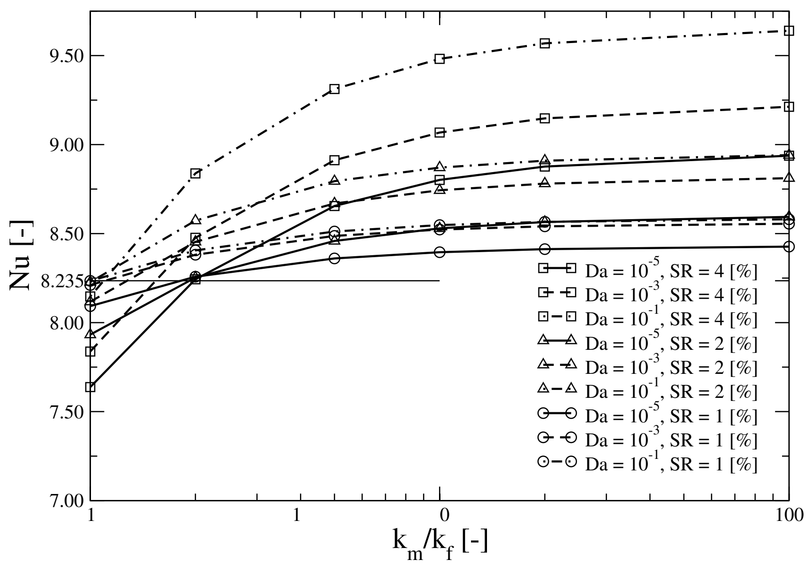

Fig. 6. Effects of PML thickness on the Nusselt number (*Re* = 1000).

3.2.2. Reynolds number effect

A small-influence of the Reynolds number on the Nusselt number for flow in tubes (see Fig. 8) is very similar to the parallel plate cases (see Section 3.1.2).

3.2.3. Effect of relative surface roughness

As it was observed for the parallel plate cases, the Nusselt number changes in tubes are greater for the high relative surface roughness cases, as shown in Fig. 9. The PML thickness effect can be understood in the same way as for the parallel plate cases. One minor difference is that the Darcy number effect for SR = 1 and 2% on the Nusselt number is smaller for tubular flow. This is due to the definition of the relative surface roughness (SR $= \frac{s}{D_h}$). In this study, we adopted the hydraulic diameter as the system length scale. The height of the surface roughness layer in parallel-plate channels is twice thicker than that in tubes resulting in a small difference in Nusselt number.

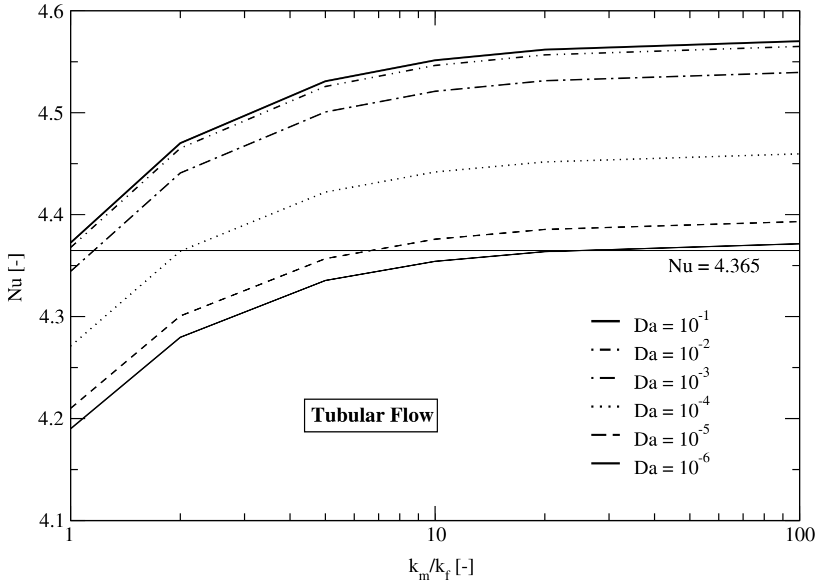

Fig. 7. Effects of PML Darcy number and thermal conductivity on the Nusselt number (Re = 1000, SR = 2%).

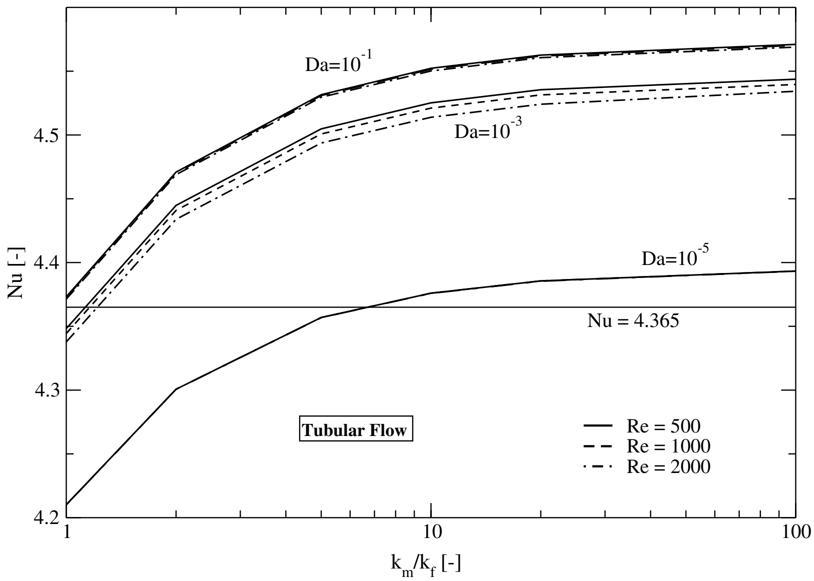

Fig. 8. Effect of the Reynolds number on the Nusselt number (SR = 2%).

3.3. Thermal dispersion effect

As mentioned in Section 1, Kuznetsov and Xiong [6] and Kuznetsov [7] investigated the thermal dispersion effect and concluded that it is negligible for low Reynolds number flows. However, they considered only low Prandtl number fluids, i.e., Pr = 0.25 and 0.7. Referring to Eq. (17), the thermal dispersion effect is a function of both Reynolds number and Prandtl number. Therefore, for high Prandtl number (e.g., $Pr_{\mathrm{oil}} \sim 1000$) in a PML region of low thermal conductivity ratio, the thermal dispersion effect could become a very important part of the heat transfer mechanism. Fortunately, thermal dispersion affects the Nusselt number in the same way as the PML thermal conductivity ratio. Hence, the effect could be simply absorbed in the thermal conductivity ratio term.

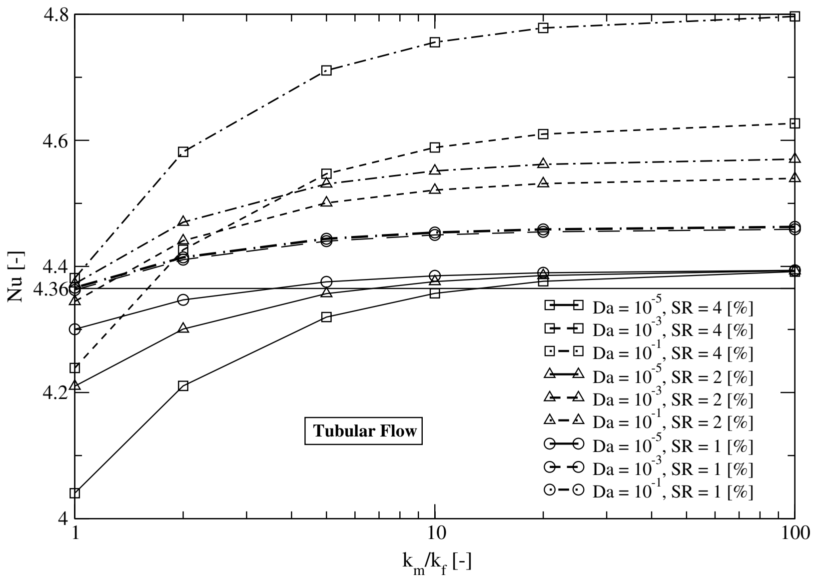

Fig. 9. Effect of PML thickness on the Nusselt number ($Re = 1000$).

4. Conclusions

The porous medium layer (PML) model introduced by Kleinstreuer and Koo [2] was extended to analyze the surface roughness effect on heat transfer in microchannels. The effects of the thermal conductivity ratio between the surface roughness layer and bulk fluid, the PML Darcy number, and relative surface roughness on temperature profile and the Nusselt number have been discussed. The new findings are summarized as follows:

- The Nusselt number can be either higher or lower than the conventional value depending on the actual surface roughness conditions, i.e., PML characteristics.
- However, the surface roughness effect on heat transfer is less significant than on momentum transfer.
- The most important parameter affecting heat transfer performance for a given relative surface roughness is the thermal conductivity ratio k_m/k_f, i.e., between PML and bulk fluid.
- The Nusselt number increases with the Darcy number, $Da = \frac{\kappa}{(H/2)^2}$ or $\frac{\kappa}{R^2}$.
- The Reynolds number effect on the Nusselt number is negligible compared to its effect on the friction factor. Hence any Reynolds number dependence observed in experimentally obtained Nusselt number correlations has to originate from effects other than surface roughness.
- Relative to the thermal parallel-plate cases, the Nusselt number for tubular flow is typically lower than the conventional value.
- For high Prandtl number fluid flow in microchannels with low PML thermal conductivity ratios, thermal dispersion may greatly influence the heat transfer mechanism.

Acknowledgements

The authors want to express their thanks to Dr. Joseph P. Archie and Sarah Archie for the endowment the McDonald-Kleinstreuer fellowship for Junemo Koo.

References

[1] J. Koo, C. Kleinstreuer, Liquid flow in microchannels:experimental observations and computational analyses of microfluidics effects, J. Micromech. Microeng. 13 (2003) 568–579.

[2] C. Kleinstreuer, J. Koo, Computational analysis of wall roughness effects for liquid flow in micro-conduits, J. Fluids Eng. 126 (2004) 1–9.

[3] G. Croce, P. D'Agaro, Numerical analysis of roughness effect on microtube heat transfer, Superlattices Microstruct. 35 (2004) 601–616.

[4] C.B. Sobhan, S.V. Garimella, A comparative analysis of studies on heat transfer and fluid flow in microchannels, Microscale Thermophys. Eng. 5 (2001) 293–311.

[5] G.L. Morini, Single-phase convective heat transfer in microchannels:a review of experimental results, Int. J. Therm. Sci. 43 (2004) 631–651.

[6] A.V. Kuznetsov, M. Xiong, Numerical simulation of the effect of thermal dispersion on forced convection in a circular duct partly filled with a Brinkman–Forchheimer

porous medium, Int. J. Numer. Methods Heat Fluid Flow 10 (2000) 488–501.
[7] A.V. Kuznetsov, Influence of thermal dispersion on forced convection in a composite parallel-plate channel, Z. Angew. Math. Phys. 52 (2001) 135–150.
[8] D.C. Tretheway, C.D. Mainhart, Apparent fluid slip at hydrophobic microchannel walls, Phys. Fluids 14 (3) (2002) 9–12.
[9] H.Y. Wu, P. Cheng, An experimental study of convective heat transfer in silicon microchannels with different surface conditions, Int. J. Heat Mass Transfer 46 (2003) 2547–2556.
[10] J.W.G. Tyrrell, P. Attart, Images of nanobubbles on hydrophobic surfaces and their interactions, Phys. Rev. Lett. 87 (17) (2001) 1–4.
[11] D.C. Tretheway, C.D. Mainhart, A generating mechanism for apparent fluid slip in hydrophobic microchannels, Phys. Fluids 16 (5) (2004) 1509–1515.
[12] J. Pfhaler, J. Harley, H. Bau, J. Zemel, Gas and liquid flow in small channels, Actuators, and Systems DSC, Micromech. Sensors 32 (1991) 49–60.
[13] X.F. Peng, G.P. Peterson, W.B.X. Frictional, flow characteristics of water flowing through rectangular microchannels, Exp. Heat Transfer 7 (1994) 249–264.
[14] G.M. Mala, D. Li, Flow characteristics of water in microtubes, Int. J. Heat Mass Transfer 20 (1999) 142–148.
[15] I. Papautsky, J. Brazzle, T. Ameel, A.B. Frazier, Laminar fluid behavior in microchannels using micropolar fluid theory, Sens. Actuators 73 (1999) 101–108.
[16] B. Xu, K.T. Ooi, N.T. Wong, W.K. Choi, Liquid flow in microchannels, in: Proc. 5th ASME/JSME Joint Thermal Engineering Conference, San Diego, CA, 1999.
[17] B. Xu, K.T. Ooi, N.T. Wong, W.K. Choi, Experimental investigation of flow friction for liquid flow in micro channels, Int. Comm. Heat Mass Transfer 27 (2000) 1165–1176.